A photonanozyme with light-empowered specific peroxidase-mimicking activity

*Sili Lin‡, Wenlong Tan‡, Pengfei Han, Xu Li, Jinzhao Li, Zhou Nie, Kun Li**

State Key Laboratory of Chemo/Biosensing and Chemometrics, College of Chemistry and Chemical Engineering, Hunan Provincial Key Laboratory of Biomacromolecular Chemical Biology, Hunan University, Changsha 410082, P. R. China

‡ These authors contributed equally to this work.

* Correspondence: kunli@hnu.edu.cn (K. L.)

Abstract

Although nanozymes have been widely developed, directly utilizing light to drive catalytic reactions like natural photoenzymes still remains challenging. Here, we propose that photonanozymes (PNZs), as a novel kind of nanozyme, exclusively possess enzyme-mimicking activity under illumination. Only in the presence of visible light, the as-synthesized TiO_2 proposed in this contribution shows excellent specificity of peroxidase-like without any oxidase- or catalase-like activity. The driving force of the light-empowered peroxidase-like photonanozymatic activity is explicated in terms of the photogenerated hot charge carriers in TiO_2 PNZs and the accompanied reactive oxygen species. The co-substrates for photonanozymatic reaction over TiO_2 PNZs facilitate the formation of the precarious and reactive peroxo-oxygen bridge between TiO_2 and H_2O_2, enabling the catalytic specificity. With the TiO_2 PNZ-based biosensing platform for visual glucose detection exemplifying the concept of the application of PNZs, this work may evoke more inspirations to explore strategies for enlarging the scope of photoenzyme mimics.

Keywords: *Photonanozyme, Titanium dioxide, Peroxidase mimics, Specificity, Biosensors*

Table of Contents

Light as a direct energy source driving photonanozymatic reactions with H_2O_2 enables TiO_2 photonanozymes to have the peroxidase-like specificity exclusively under illumination. Photogenerated hot charge carriers and the accompanied reactive oxygen species are responsible for light-empowered photonanozymatic activity. Co-substrates are conducive to the formation of the photo-reactive peroxo-oxygen bridge bond between TiO_2 and H_2O_2, which specifically allows the peroxidase-like activity.

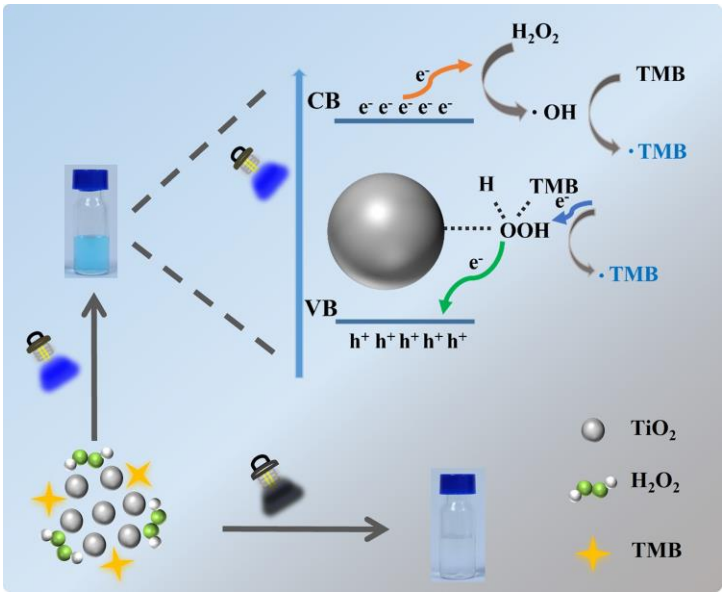

1. Introduction

Biocatalysis has become a green tool in chemical synthesis because only generally mild reaction conditions are required and enzymes have high specificity and selectivity.[1, 2] In the past decades, the strategy of combining enzymatic catalysis and chemical catalysis is substantially increased to achieve higher yields, lower costs, and better selectivity.[3, 4] However, the inconsistency of the reaction conditions hinders the improvements of bio- and chemo-catalysis hybridized systems,[5] especially for the cooperation between

biocatalysis and photocatalysis, which is a promising means because light can be easily obtained as a clean and sustainable energy source.[6, 7] DNA photolyases,[8, 9] protochlorophyllide oxidoreductase,[8, 10] and fatty acid photodecarboxylases[11, 12] are only three known natural light-dependent enzymes, i.e., the so-called photoenzymes.[13] These photoenzymes per se exploit light energy without any assistance from other co-catalysts or modification of the natural enzymes. However, the scope of photoenzymatic catalysis is limited to reactions that are found in nature, making the exploration of photo-biocatalysis still challenging.[14]

Introducing light into non-light-dependent enzymatic catalysis is an effective way to expand the types of enzymes for light energy utilization. To this purpose, versatile approaches have been developed. For example, enzymes that are coupled with chemical photocatalysts, including homogeneous molecular catalysts[15, 16] and heterogeneous nanocatalysts,[17] enable cascade reactions producing compounds more effectively than can the same catalysts used sequentially. Another effective and simple method is driving the indirect transfer of photoinduced electrons to an enzyme, where the photochemical regeneration of cofactors plays a crucial role.[18, 19] Moreover, the reformation of existing enzymes through nongenetic (e.g., modification with a photosensitizer[20, 21]) or genetic (e.g., directed evolution[22, 23]) engineering facilitates the utilization of light energy. Overall, the above strategies still require natural enzymes, which are generally expensive and sensitive to reaction conditions.

As a kind of artificial analogue of enzymes, nanozymes are inorganic nanomaterials that possess enzyme-mimicking kinetic behaviors in the conversion of enzyme substrates to products,[24, 25] allowing them to be widely used in environmental remediation,[26] molecular detection,[27, 28] as well as biomedicine and therapeutics.[29] However, most of the current existing light/nanozyme systems are ascribed to photo-activated nanozymes or photo-responsive nanozymes.[30-32] The essential of them is that only the ligand molecules or modification materials around the nanozymes are controlled by light for strengthening

or weakening the catalytic activity, while the nanozymes themselves always hold the intrinsic property for catalysis.[33, 34] In addition, unlike photocatalysis that happened over photoenzymes, in the above mentioned photo-controlled thermocatalytic systems, light is never be employed as the direct source of energy for driving the chemical conversion, although some nanomaterials (such as semiconductors and precious metal nanoparticles) are accompanied with photogeneration of reactive oxygen species under light stimulation.

Inspired by the nanomaterial-based photocatalysis, we propose a novel kind of nanozyme that possesses enzyme-mimicking activity only under illumination, while is completely non-active for thermo-catalysis in the dark. In this contribution, as the counterpart of photoenzymes, the photocatalytic nanomaterials that utilize light as the sole driving force and mimic enzymatic activity are termed photonanozymes (PNZs), following the same naming pattern as enzymes and nanozymes. Considering anatase titanium dioxide (TiO_2)-based materials are known to particularly occupy an outstanding position in various photocatalysis,[35, 36] here we demonstrate that the decomposition of H_2O_2 on TiO_2 for the oxidation of a variety of substrates is exclusively empowered by light. TiO_2 PNZs solely possess the peroxidase-like reactivity under the light as O_2 molecules cannot be activated by illuminating TiO_2 PNZs. The study on structural and optical features of TiO_2 PNZs in the presence of substrates substantiates the formation of a peroxo-oxygen bridge between TiO_2 and H_2O_2, which is further proved to be responsible for the catalytic specificity. Lastly, as a proof of concept, the TiO_2 PNZs-based biosensor is constructed for sensitive colorimetric detection of glucose, which holds great promise in biosensing applications.

2. Results and Discussion

2.1. Peroxidase-like activity of TiO_2 PNZs

To prepare TiO_2 PNZs, nanostructured TiO_2 particles were synthesized via a classical hydrothermal method.[38] The morphology and size distribution of the TiO_2 PNZs were

investigated by transmission electron microscopy (TEM), as is shown in Figure S1A. The particle size of TiO_2 PNZs is in the range of 10-20 nm, which is consistence with the result of dynamic light scattering (DLS) measurements indicating a diameter around 50 nm for little accumulation in water (Figure S1B). The obtained anatase TiO_2 was proved by the X-ray diffraction pattern (XRD) test (Figure S1C), confirming the successful synthesis of TiO_2 PNZs. Finally, the optical property of the prepared TiO_2 PNZs was studied by the diffuse reflectance ultraviolet-visible (DRUV-vis) absorption spectrum (Figure S1D), which shows that the TiO_2 PNZs interact with photons majorly at the wavelength shorter than 390 nm.

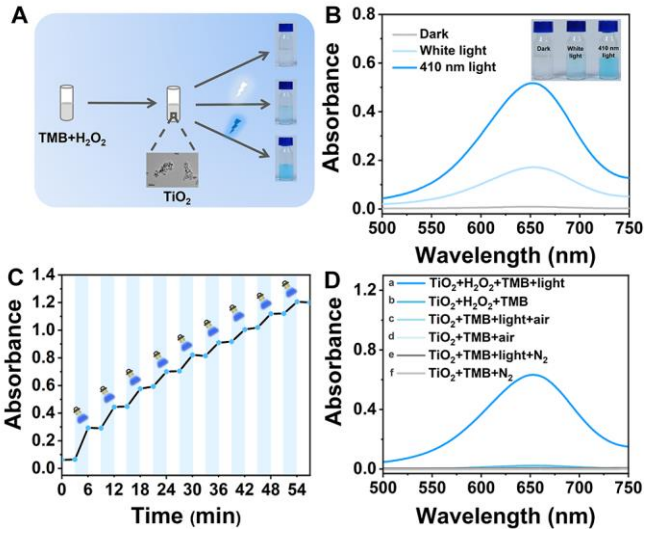

Figure 1. Peroxidase-like activity of TiO_2 photonanozymes (PNZs). (A) Schematic diagram of the peroxidase activity of TiO_2 PNZs; (B) The absorbance of oxTMB representing the peroxidase activity of TiO_2 PNZs under different light sources (blank, white light, 410 nm LED light source, power density: 38.3 $mW \cdot cm^{-2}$); (C) UV-visible absorption spectra of different reaction systems. Experimental conditions: reaction time was 30 min with the light irradiation of 410 nm. (D) Staircase-like behavior of peroxidase-mimicking activity of TiO_2 PNZs with the continuous on and off of the blue 410 nm LED (interval 3 min). In panels B, C, and D, the reactions were conducted with 208 μM TMB, 10 mM H_2O_2, and 25 μg·mL−1 TiO_2 PNZs in 0.2 M acetate buffer (pH 4.0). The absorbances were recorded for oxTMB at 652 nm.

To verify the photo-dependent enzyme-like catalytic activity of the TiO_2 PNZs, we conducted a typical chromogenic reaction, in which the colorless 3,3′,5,5′-tetramethylbenzidine (TMB) was catalytically oxidized to the blue oxidation state of TMB

(oxTMB) by hydrogen peroxide (H_2O_2) in presence of TiO_2 under light (Figure 1A). By recording the absorbance of oxTMB at 652 nm,[39] we find that in the absence of light, TiO_2 PNZs cannot trigger the interaction between H_2O_2 and TMB. However, if the irradiation from white light was introduced, an obvious increase of the absorption at 652 nm is observed, indicating the photo-dependent enzyme-like activity (Figure 1B). Furthermore, the dependence of the catalytic activity on the light wavelength was studied. In the visible-light regime, as the wavelength goes longer, the catalytic activity of peroxidase decreases gradually (Figure S2A). The wavelength-dependent photocatalytic results were further confirmed by the chronoamperometric response experiment (Figure S2B). Accordingly, to investigate the peroxidase-like activity of TiO_2 PNZs under visible light, 410 nm was selected as the excitation wavelength for subsequent studies.

A light "on-off" experiment was performed to further confirm the peroxidase-like activity of the TiO_2 PNZs is photo-dominated. We find that only under the light irradiation, the absorbance at 652 nm of oxTMB increases significantly, which keeps constant while the light irradiation turns off (Figure 1C and Figure S3). This staircase-like behavior indicates that light is an essential factor in the photonanozymatic performance of TiO_2 PNZs. Furthermore, the photocatalytic activity after several catalytic cycles were maintained (Figure S4), indicating that the TiO_2 PNZs exhibited good stability without undergoing damage and loss of activity.

Six different reaction systems were designed to probe the specificity of the proposed PNZs. As shown in Figure 1D, compared with other reaction systems, TiO_2 PNZs can only catalyze the oxidation of TMB in the presence of H_2O_2 under visible-light irradiation, where a significant increase of the absorption at 652 nm is noted (curve a). As a comparison, TiO_2 PNZs cannot catalyze the reaction between H_2O_2 and TMB under the dark (curve b). This confirms the photonanozymatic reaction is a kind of photocatalysis mimicking photoenzymes, rather than photo-enhanced thermocatalysis like light-responsive nanozymes. Furthermore, due to the incapable of exciting TiO_2 under 410 nm light

irradiation in the absence of H_2O_2, curves c and d show negligible absorbance under either light irradiation or the dark. Thus, the possibility of oxidase-mimicking activity is preliminarily excluded for the TiO_2 PNZs. We also challenged the catalytic activity toward TMB oxidation of TiO_2 PNZs in the absence of O_2 and H_2O_2, which suggests that TiO_2 PNZs themselves, no matter with or without photo-excited hot charge carriers, cannot drive the formation of oxTMB (curve e and f). Moreover, it should be pointed out that TiO_2 is the critical catalyst in this system since the mixture of TMB and H_2O_2 without the addition of TiO_2 does not generate oxTMB (Figure S5). Above results suggest that TiO_2, light, and H_2O_2 are all necessary substances for the photonanozymatic reaction. Thus, this further inspired us to investigate the catalase-like activity of TiO_2 PNZs. By comparing the absorption intensity of the characteristic peak of H_2O_2 at 240 nm before and after light irradiation, it is found that light does not influence the stability of H_2O_2 (Figure S6A) and no bubbles appeared in the reaction solution, indicating that TiO_2 NPs have no catalase-mimicking activity. Furthermore, the possible partial self-decomposition of H_2O_2 under light irradiation will not affect the photonanozymatic reaction (Figure S6B). These results substantiate TiO_2 PNZs possess a unique light-empowered photoenzyme-like activity with the peroxidase-mimicking specificity.

2.2. Kinetics analysis for TiO_2 PNZs

TiO_2 PNZs display excellent light-dependent peroxidase-like activity. Furthermore, the light-dependent peroxidase-like reaction process follows the conventional enzymatic dynamic regulation of the Michaelis–Menten equation $v = V_{max}[S]/ (K_m + [S])$, where v is the initial velocity, $[S]$ is the concentration of substrate, V_{max} refers to the maximum reaction velocity, and K_m is defined as the Michaelis−Menten constant, and was monitored by testing the absorption of oxTMB. Therefore, steady-state kinetics of TiO_2 PNZs was quantitatively studied on the basis of the absorbance value of oxTMB at 652 nm. As expected from Figure 2, the peroxidase-like activity of TiO_2 PNZs fits the typical Michaelis−Menten equation well for both TMB and H_2O_2. With the double reciprocal

Lineweaver−Burk diagram (Figure 2B and Figure 2D), the K_m values of TiO_2 PNZs for TMB and H_2O_2 are calculated as 0.08 mM and 7.16 mM, respectively. These parameters reach the level of horseradish peroxidase (HRP) and are lower than that of the most recently-developed nanozymes (Table S1), indicating TiO_2 PNZs possess a strong affinity towards both TMB and H_2O_2. In addition, the V_{max} values of TiO_2 PNZs for TMB and H_2O_2 are similar to that of HRP, suggesting the fast rate of such a catalytic reaction. Accordingly, the Michaelis−Menten-style kinetics guarantees that the TiO_2 PNZ with unique light-dependent peroxidase-like activity is a kind of enzyme mimic, that is, photonanozyme.

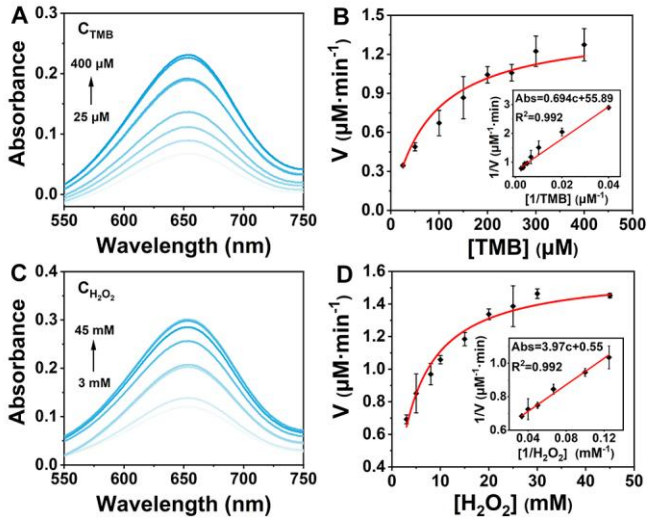

Figure 2. Kinetic assay of TiO_2 PNZs. (A) UV-vis absorption spectra of peroxidase-like TiO_2 PNZs catalyzed H_2O_2 (10 mM) with TMB of different concentrations. (B) Steady-state kinetic assay of TiO_2 PNZs by varying the concentration of TMB. Inset: Lineweaver−Burk plot of photocatalytic activity of the TiO_2 PNZs with H_2O_2 as the substrate. (C) UV-vis absorption spectra of peroxidase-like TiO_2 PNZs catalyzed TMB (208 μM) with H_2O_2 of different concentrations. (D) Steady-state kinetic assay of TiO_2 PNZs by varying the concentration of H_2O_2. Inset: Lineweaver−Burk plot of photocatalytic activity of the TiO_2 PNZs with TMB as the substrate. In all experiments, TiO_2 was 25 μg·mL^{-1} diluted in 0.2 M acetate buffer (pH 4.0).

In order to investigate the substrate versatility of TiO_2 PNZs, 2,2′-azino-bis (3-ethylbenzothiazoline-6-sulfonic acid) (ABTS) and o-phenylenediamine (OPD) were also selected as chromogenic substrates to examine the peroxidase-like activity. Compared with that using TMB as a substrate, it is seen that the K_m value is close (Section 7, Supporting Information). Thus, TiO_2 PNZs holding a light-empowered peroxidase-like activity can

drive the reaction between H_2O_2 and various co-substrates, which is consistent with other reported peroxidase mimics.

2.3. Mechanism of the light-empowered peroxidase-like activity

To interpret the mechanism of TiO_2 nanoparticles as photonanozymes, we first investigated the influence of H_2O_2 and the co-substrate on the structural and optical properties of TiO_2 (Section 8, Supporting Information). The X-ray diffraction (XRD) spectra show the diffraction peaks of the as-synthesized TiO_2 and the hydrogen peroxide-treated TiO_2 (P-TiO_2) are consistent with that of anatase TiO_2 (Figure S9), which indicates that the crystal structure of anatase TiO_2 retains after the incubation with H_2O_2 and acetate buffer. DRUV-vis absorption spectra of the obtained samples (Figure S10) demonstrate the P-TiO_2 sample possesses a certain reflectance in the visible-light regime around 410 nm, suggesting a reduced bandgap energy of P-TiO_2. The increase of photocurrent in the electrochemical measurements for TiO_2 after adding H_2O_2 under 410 nm light irradiation indicates that TiO_2 can drive the redox reaction of H_2O_2 (Figure S11). Moreover, we carried out the electron spin resonance (ESR) spectroscopy for the as-synthesized TiO_2 and P-TiO_2. The oxygen vacancy concentration in the P-TiO_2 is significantly reduced comapring to the TiO_2 sample (Figure S12), proving the adsorption of H_2O_2 on the surface of TiO_2 and its decomposition towards oxygen species. All above results indicate the successful formation of P-TiO_2, in which the structural and optical properties are interrelated.

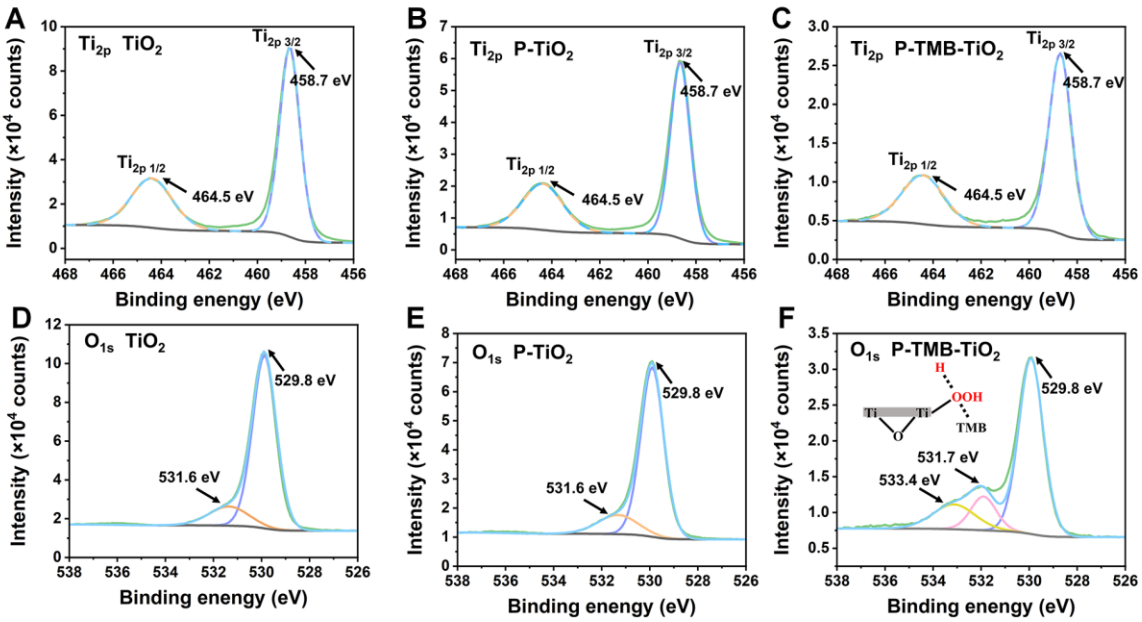

Figure 3. XPS spectra for the as-synthesized TiO_2 and hydrogen peroxide-treated TiO_2 (P-TiO_2). Ti_{2p} (A) and O_{1s} (B) spectral signals of TiO_2; Ti_{2p} (C) and O_{1s} (D) spectral signals of P-TiO_2; Ti_{2p} (E) and O_{1s} (F) spectral signals of P-TMB-TiO_2. (Green, blue, and gray curves correspond to raw, peak-fitted, and background spectra, respectively. Others show separated peaks.)

However, the decomposition mechanism of hydrogen peroxide (H_2O_2) by TiO_2 under illumination is still controversial.[40-42] To figure out the bonding status of the decomposed H_2O_2 on the surface of TiO_2, we further performed X-ray photoelectron spectroscopy (XPS) for TiO_2 and P-TiO_2. Figures 3A and 3B reveal that the Ti_{2p} spectra of TiO_2 and P-TiO_2 are composed of peaks belonging to Ti_{2p} 3/2 and Ti_{2p} 1/2 at 458.7 eV and 464.5 eV, respectively, indicating that Ti ions have an octahedral structure. Moreover, in the O_{1s} XPS spectra of TiO_2 and P-TiO_2 (Figures 3C and 3D), the peaks of Ti–O (529.8 eV) and of Ti–OH (531.6 eV) are observed. By comparing the integrated area of the O_{1s} XPS spectra of TiO_2 and P-TiO_2 peak centered at 531.6 eV, we found the oxygen content of TiO_2 after H_2O_2 treatment is ~2.0% higher than that of as-synthesized TiO_2 (calculated by the integral of the entire peak area). Accordingly, the treatment of TiO_2 by H_2O_2 increases the content of the hydroxyl (–OH) group on the surface of TiO_2, as expected. This phenomenon should be attributed to the decomposition of H_2O_2 after the adsorption on TiO_2.[43] Moreover, the

absence of Ti–O–OH peak in the O_{1s} spectra further confirms that the homolytic dissociation of H_2O_2 towards –OH by anatase TiO_2, which is consistent with previous report.[44]

After successfully proving that the H_2O_2 is decomposed to form –OH groups adsorbed on the TiO_2, it is critical to figure out whether the adsorbed –OH groups of P-TiO_2 affect the peroxidase-like photonanozymatic reaction (Section 9, Supporting Information). After drying P-TiO_2 at different temperatures, the blue-shift of the DRUV-vis absorption spectra spectroscopy with the increased temperature indicates that the –OH groups adsorbed on the surface of TiO_2 tend to dissociate at higher temperatures (Figure S13A). However, the adsorbed –OH groups on P-TiO_2 are not responsible for the TMB oxidation under 410 nm light because TMB can not be oxidized if only P-TiO_2 is employed (Figure S13B). Furthermore, the absence of the ESR signal of superoxide ($O_2^{\bullet-}$) radical further indicates that $O_2^{\bullet-}$ radical is not generated under light illumination (Figure S14). Therefore, the extra addition of H_2O_2 is necessary for TMB oxidation, while the adsorbed H_2O_2 which has homogeneously cleaved towards –OH groups cannot drive the reaction. This guarantees the P-TiO_2 holds the behavior of peroxidase-like rather than oxidase-like photonanozymatic activity, thereby achieving its catalytic specificity.

Thus, for exploring the role of TiO_2 PNZs in the reaction between TMB and H_2O_2, the study on the adsorption of TMB on P-TiO_2 is a prerequisite step. We performed the X-ray photoelectron spectroscopy (XPS) for TiO_2 that was treated with H_2O_2 and TMB consequently (P-TMB-TiO_2). Figure 3E shows that the Ti_{2p} spectrum of P-TMB-TiO_2 is composed of two peaks at 458.7 eV (belonging to Ti_{2p} 3/2) and 464.5 eV (belonging to Ti_{2p} 1/2), which is consistent with the XPS results of the TiO_2 and P-TiO_2. In the O_{1s} XPS spectrum of P-TMB-TiO_2 (Figure 3F), the peak at 529.8 eV indicates the presence of Ti–O, while the separated peak at 531.7 eV should be attributed to Ti–OH. The peak at 533.4 eV is an obvious Ti–O−OH peak.[43 44] To investigate the status of oxygen bridge bond in Ti–O−OH and the evolution of the surface species on P-TMB-TiO_2 under TMB oxidation

reaction conditions, we performed Raman measurements in the atmosphere for TiO_2 PNZs with a series of solutions (Figure S15). For P-TMB-TiO_2, the Raman band at 885 cm^{-1} belonging to Ti–O–OH peak is observed. This is ascribed to the peroxo (O–O) functional group from H_2O_2, which forms the peroxo-titanium bond (Ti–O–OH) through the interaction with a Ti atom.[40-42] Interestingly, for P-TiO_2, the Ti–O–OH bond is not detected by Raman, which is consistent with the XPS results (Figure 3D). This indicates that TMB helps the heterolytic cleavage (towards –O–OH and –H) rather than the homolytic cleavage (towards –OH) of H_2O_2, promoting the production of Ti–O–OH as a bridge between TMB, H_2O_2, and TiO_2.[45] Accordingly, from the XPS and Raman results, we rationally speculate that the cracking of H_2O_2 on TiO_2 is depressed with the addition of TMB by forming a hydrogen bond, reaching a competitive adsorption equilibrium between TMB and H_2O_2 on the surface of TiO_2. In addition, the above results suggest that Ti–O–OH is extremely unstable and reactive, which may only shortly exist in the solution system.

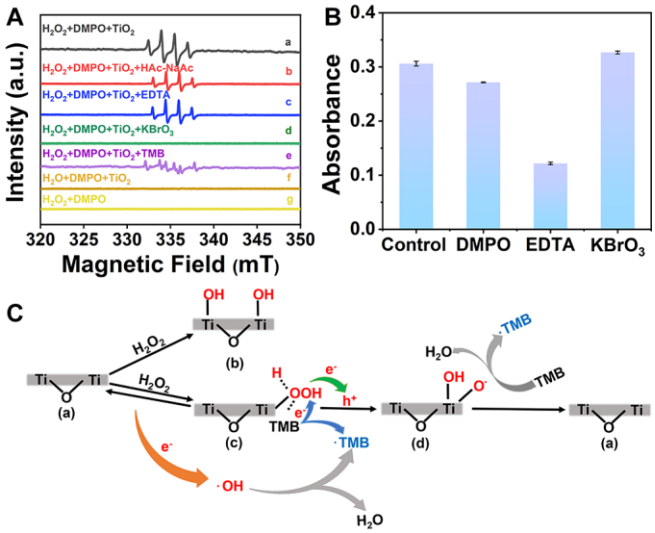

Figure 4. Proposed mechanism for the light-empowered peroxidase-like photonanozymatic reaction of TiO_2 PNZs. (A) ESR spectra of different DMPO-TiO_2 systems under light irradiation. •OH was trapped in an aqueous solution. (B) The UV-vis absorption of oxTMB representing the photocatalytic activity of TiO_2 for TMB oxidation under light illumination with the addition of different scavengers (DMPO, EDTA, and $KBrO_3$). In panels A and B, the concentrations of reactants are as follows. H_2O_2: 10 mM, TMB: 208 μM, TiO_2 PNZs: 25 μg mL^{-1}, Scavengers: 10 mM. (C) Plausible reaction pathway for TiO_2 PNZs. The colorful arrows (orange, green, and blue) present different charge carrier transmission routes.

Above results demonstrate the optical and structural features of the substrates adsorbed TiO_2 PNZs, suggesting that H_2O_2 plays an important role in promoting charge transfer and improving the photocatalytic performance of TiO_2 PNZs under illumination. It is generally accepted that the photocatalytic oxidation is ascribable to the reactive oxygen species.[40, 44] Accordingly, we used DMPO as a free radical scavenger in the ESR spectroscopy analysis for reactions under light illumination.[46] When H_2O_2 is added to TiO_2 PNZs, the ESR signal of •OH radical appears a characteristic quartet signal (1:2:2:1) (Figure 4A, curve a), while the parallel reaction displayed no signals (Figure 4A, curve f and g). The same ESR signal in acetate buffer (Figure 4A, curve b) substantiates the existence of •OH radicals in the peroxidase-like photonanozymatic reaction condition. Moreover, the formation of •OH radicals was further confirmed by the oxidation of terephthalic acid (TA), as •OH radicals can convert terephthalic acid to 2-hydroxyterephthalic acid (Figure S16). Meanwhile, we also performed the ESR test of free •OH for different reaction systems in the dark (Figure S17), which further verifies that •OH is only present during the photocatalytic reaction.

We next aimed to investigate the source of the generation of •OH for figuring out the photoenzymatic mechanism of TiO_2 PNZs in the presence of H_2O_2 and TMB. For nanozymes, most mechanism studies have shown that the peroxide properties of peroxidase mimics are generally produced by catalyzing H_2O_2 to produce •OH.[40, 44] Photogenerated electrons of semiconductor photocatalysts are easily excited from the valence band (VB) to the conduction band (CB). Therefore, for both TiO_2 with and without H_2O_2, the comparison of transient open-circuit photovoltage decay (OCP) measurements under 410 nm illumination and in the dark was carried out first (Figure S18). The results suggest that H_2O_2 can decrease the recombination rate of photo-excited charge carriers generated on TiO_2 under light irradiation.[47] Consequently, hot charge carriers are transmitted to the adsorbed H_2O_2, which generates •OH radicals.

Furthermore, we added free radical scavenger agents DMPO into the system of TiO_2

PNZs-catalyzed TMB oxidation by H_2O_2 to verify the influence of free radicals on the catalytic properties of PNZs (Section 11.4, Supporting Information). However, the absorbance of oxTMB only slightly decreased during the entire reaction, as shown in Figure 4B and Figure S19A. Obviously, free •OH radicals may not be the only reason for the oxidation of TMB under the 410 nm light. Hence, we were inspired by the above results to further explore the roles of hot carriers in this peroxidase-like photonanozymatic system. The hot hole scavenger EDTA and electron scavenger $KBrO_3$ were added into the reaction solution, respectively (Figure S19B, C).[48] On one hand, EDTA was used as an electron sacrificial agent to clear the holes and the generation of •OH radicals was measured by ESR spectroscopy using DMPO as a free radical trapped agent (Figure 4A, curve c). A characteristic quartet signal (1:2:2:1) is also clearly shown in the ESR spectra, indicating the generation of •OH radicals in the presence of hot electrons. Although, once the holes are cleared with the addition of EDTA, the generation of oxTMB is also decreased (Figure 4B). Thus, it is rationally speculated that the hole may be another important initiator for TMB oxidation. On the other hand, $KBrO_3$ was used as a hole sacrificial agent to clear hot electrons (Figure 4A, curve d). With DMPO as a radical trapping agent for ESR spectroscopy, no •OH radical signal peak is shown. This may result from the consumption of hot electrons by $KBrO_3$, which depresses the trapping of hot electrons by H_2O_2 and the generation of •OH radicals. Simultaneously, the holes are able to transfer to the adsorbed Ti−O−OH bond on the TiO_2 surface, generating adsorbed •O radicals.[49] The addition of $KBrO_3$ clears the hot electrons, but brings an increase of the TMB oxidation, as is shown in Figure 4B. This further confirms that holes are an essential source for the generation of oxTMB. Therefore, in addition to hot electrons that are absorbed by H_2O_2 to form •OH radicals for driving the POD-like photonanozymatic reaction, hot holes can also attack Ti−O−OH to generate adsorbed •O radicals (as ESR detects no •OH radical signal, shown in Figure 4A, curve e), further producing •TMB free radicals.[50] Above results explicate that both two kinds of hot carriers play vital roles in the light-empowered reactivity of TiO_2 as

a POD-like PNZs.

Thus, the properties of peroxidase-like TiO_2 PNZs are dominated by the combination of oxidative activities from both hot electrons derived •OH radicals and hot holes. Therefore, the mechanism of the light-empowered TiO_2 PNZs with a POD-like catalytic specificity is proposed (Figure 4C). First, H_2O_2 can be adsorbed on anatase TiO_2 to form homo-cleaved −OH groups on the TiO_2 surface (a to b),[40-42, 49, 51, 52] hindering the activation of O_2 by occupying the oxygen vacancies of TiO_2. At the same time, H_2O_2 also undergoes heterolytic cleavage to generate a peroxo-oxygen bridge (Ti−O−OH) between TiO_2 and H_2O_2 in the presence of TMB, which forms a hydrogen bond with H_2O_2 (a to c). Second, at 410 nm light irradiation, the hot electrons excited on TiO_2 directly transfer to the adsorbed H_2O_2 (orange arrow) to produce •OH radicals (c to a), which is further reduced to water by TMB. Meanwhile, in structure c, TMB releases an electron to the peroxo-oxygen bridge (blue arrow) to generate •TMB radicals (c to d). Finally, hot holes directly capture electrons from the peroxo-oxygen bridge (green arrow) to generate adsorbed •O radicals, while the adsorbed •O radicals on TiO_2 interact with another TMB molecule, allowing a second way to the formation of •TMB radicals and the recovery of TiO_2 (d to a). In summary, H_2O_2 is decomposed by TiO_2 PNZs to yield water at 410 nm light irradiation, enabling the formation of oxTMB**.**

2.4. Construction of biosensors for glucose detection

Based on the excellent peroxidase-mimicking property of TiO_2 PNZs, we built a GOx-TiO_2 PNZs-TMB system for the determination of glucose (Figure 5A). To improve the performance of the biosensor, the concentration of photonanozymes, pH of the reaction system, reaction temperature, and incubation time were optimized (Figure S20). Under the optimized conditions, as the glucose concentration increases, the absorbance at 652 nm rises accordingly, along with an obvious color variation from colorless to blue (Figure 5B). As depicted in Figure 5C, a good linear relationship between the absorbance at 652 nm and glucose concentration is established in the range from 0.5 to 100 μM with R^2=0.995. The

limit of detection (LOD) for glucose in acetate buffer was calculated to be 0.497 μM at a signal-to-noise ratio (S/N) of 3, indicating the high sensitivity of the TiO_2 PNZs for glucose detection. In order to evaluate the selectivity of the proposed colorimetric sensor, a variety of common analogues and ions were tested. In the case of the same substrate concentration, only glucose produces a significant change in solution color whereas the reactions with the above substances stay colorless (Figure 5D), indicating the proposed sensing system displays a good identification specificity for glucose.

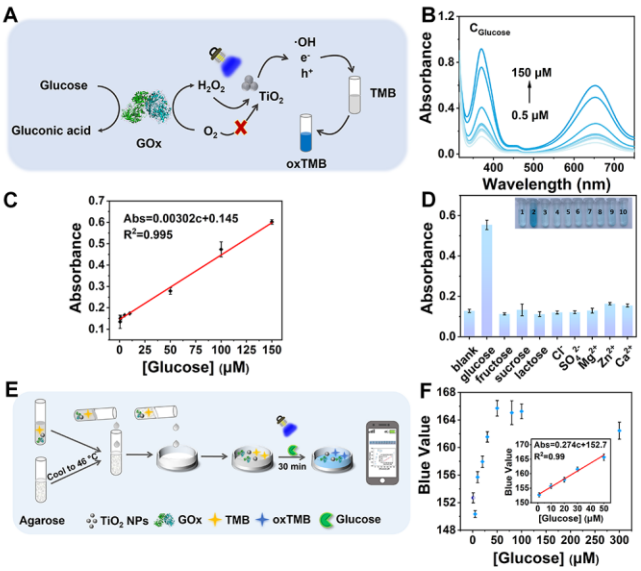

Figure 5. Glucose sensing with POD-like TiO_2 PNZs. (A) Schematic illustration of colorimetric detection of glucose. (B) The UV-visible absorption spectra of oxTMB with different glucose concentrations. (C) The linear calibration plots for glucose detection (Inset: the corresponding color changes). (D) Selectivity of TiO_2 PNZs sensor. Inset: the photograph of the color changes of different substances. All the concentrations are 100 μM. (E) Schematic diagram of agarose hydrogel colorimetric detection of glucose. (F) Linear calibration plot between blue channel value and glucose concentrations. TMB: 400 μM, GOx: 1.25mg·mL^{-1}, TiO_2 NPs: 250 μg·mL^{-1}, 0.2 M acetate buffer solution (pH 4.5), the concentration of glucose is from 1 to 300 μM, 410 nm light irradiation for 30 min.

In order to broaden the practicality of the GOx-TiO_2 PNZs-TMB colorimetric biosensing system, we constructed an agarose-based hydrogel colorimetric platform for glucose detection (Figure 5E). To assess the potential of the hydrogel biosensing system, the photograph of the final reaction solution was captured by a smartphone (iPhone XR).

The three optical channels (Red, Green, and Blue) levels of the resulting photograph were extracted with a smartphone application (Universal color) which could output the RGB value corresponding to the color of the photograph (Figure 5F and Figure S21). The results indicate that all of the three-channel levels increase linearly with the increase in glucose concentration. By using the blue channel, the best linear relationship ($R^2 = 0.990$) between the blue value and glucose concentration was obtained in the range of 1 to 50 μM with a LOD of 8.8 μM (Figure 5F). The best linear performance of the blue channel is attributed to the characteristic absorbance of oxTMB at 652 nm, which corresponds to the blue color in the spectrum. These results indicate that the proposed biosensing platform is expected to achieve the visualization and quantitative evsaluation for glucose in resource-limited areas.

3. Conclusion

In summary, the specific peroxidase-mimicking property of TiO_2 PNZs has been demonstrated exclusively under light irradiation. TiO_2 PNZs do not exhibit oxidase-like or catalase-like activity, attesting to the catalytic specificity. We elucidate that the adsorption of H_2O_2 on the surface induces the modification of optical and structural property of TiO_2 PNZs, while the presence of the other co-substrate (e.g., TMB) facilitates a competitive adsorption performance between TMB and H_2O_2. Furthermore, the delicate equilibrium and reactive bond are easily broken by the hot electrons and hot holes that excited on TiO_2 PNZs under irradiation. The driving force of the POD-like photonanozymatic reaction is corroborated to be the light energy absorbed by TiO_2 PNZs. In addition, a cascade biosensing platform was established on the basis of TiO_2 PNZs for colorimetric sensing of glucose in a simple and visual way. This study exemplifies an efficient and cost-effective photoenzyme-mimicking strategy, which extends the scope of photoenzymatic reactions and the field of nanozymes.

Supporting Information

Supporting Information is available from the author on request.

Acknowledgements

S.L. and W.T. contributed equally to this work. This research was financially supported by the National Natural Science Foundation of China (22074038, 21807032), the Natural Science Foundation of Hunan Province (2019JJ30007), and the Fundamental Research Funds for the Central Universities.

Conflict of Interest

The authors declare no conflict of interest.

Data Availability Statement

The data that support the findings of this study are available from the corresponding author upon reasonable request.

References

1. Sheldon, R. A.; Woodley, J. M., Role of Biocatalysis in Sustainable Chemistry. *Chem. Rev.* **2018,** *118*, 801-838.
2. Bornscheuer, U. T.; Huisman, G. W.; Kazlauskas, R. J.; Lutz, S.; Moore, J. C.; Robins, K., Engineering the third wave of biocatalysis. *Nature* **2012,** *485*, 185-194.
3. Groger, H.; Hummel, W., Combining the 'two worlds' of chemocatalysis and biocatalysis towards multi-step one-pot processes in aqueous media. *Curr. Opin. Chem. Biol.* **2014,** *19*, 171-179.
4. Ellis, L. D.; Rorrer, N. A.; Sullivan, K. P.; Otto, M.; McGeehan, J. E.; Roman-Leshkov, Y.; Wierckx, N.; Beckham, G. T., Chemical and biological catalysis for plastics recycling and upcycling. *Nat. Catal.* **2021,** *4*, 539-556.
5. Rudroff, F.; Mihovilovic, M. D.; Gröger, H.; Snajdrova, R.; Iding, H.; Bornscheuer, U. T., Opportunities and challenges for combining chemo- and biocatalysis. *Nat. Catal.* **2018,** *1*, 12-22.
6. Marzo, L.; Pagire, S. K.; Reiser, O.; Konig, B., Visible-Light Photocatalysis: Does It Make a Difference in Organic Synthesis? *Angew. Chem., Int. Ed.* **2018,** *57*, 10034-10072.
7. Qiu, X.; Zhang, Y.; Zhu, Y.; Long, C.; Su, L.; Liu, S.; Tang, Z., Applications of Nanomaterials

in Asymmetric Photocatalysis: Recent Progress, Challenges, and Opportunities. *Adv. Mater.* **2021,** *33*, e2001731.
8. Begley, T. P., Photoenzymes: A Novel Class of Biological Catalysts. *Acc. Chem. Res.* **1994,** *27*, 394-401.
9. Sancar, A., Mechanisms of DNA Repair by Photolyase and Excision Nuclease (Nobel Lecture). *Angew. Chem., Int. Ed.* **2016,** *55*, 8502-8527.
10. Zhang, S.; Heyes, D. J.; Feng, L.; Sun, W.; Johannissen, L. O.; Liu, H.; Levy, C. W.; Li, X.; Yang, J.; Yu, X.; Lin, M.; Hardman, S. J. O.; Hoeven, R.; Sakuma, M.; Hay, S.; Leys, D.; Rao, Z.; Zhou, A.; Cheng, Q.; Scrutton, N. S., Structural basis for enzymatic photocatalysis in chlorophyll biosynthesis. *Nature* **2019,** *574*, 722-725.
11. D Sorigué, B. L., S Cuiné, An algal photoenzyme converts fatty acids to hydrocarbons. *Science* **2018,** *357*, 903-907.
12. Heyes, D. J.; Lakavath, B.; Hardman, S. J. O.; Sakuma, M.; Hedison, T. M.; Scrutton, N. S., Photochemical Mechanism of Light-Driven Fatty Acid Photodecarboxylase. *ACS Catal.* **2020,** *10*, 6691-6696.
13. Björn, L. O., Photoenzymes and Related Topics: An Update. *Photochem. Photobiol.* **2018,** *94*, 459-465.
14. Schmermund, L.; Jurkas, V.; Ozgen, F. F.; Barone, G. D.; Buchsenschutz, H. C.; Winkler, C. K.; Schmidt, S.; Kourist, R.; Kroutil, W., Photo-Biocatalysis: Biotransformations in the Presence of Light. *ACS Catal.* **2019,** *9*, 4115-4144.
15. Litman, Z. C.; Wang, Y.; Zhao, H.; Hartwig, J. F., Cooperative Asymmetric Reactions Combining Photocatalysis and Enzymatic Catalysis. *Nature* **2018,** *560*, 355-359.
16. Huang, X.; Wang, B.; Wang, Y.; Jiang, G.; Feng, J.; Zhao, H., Photoenzymatic enantioselective Intermolecular Radical Hydroalkylation. *Nature* **2020,** *584*, 69-74.
17. Zhang, S.; Zhang, Y.; Chen, Y.; Yang, D.; Li, S.; Wu, Y.; Sun, Y.; Cheng, Y.; Shi, J.; Jiang, Z., Metal Hydride-Embedded Titania Coating to Coordinate Electron Transfer and Enzyme Protection in Photo-enzymatic Catalysis. *ACS Catal.* **2020,** *11*, 476-483.
18. Emmanuel, M. A.; Greenberg, N. R.; Oblinsky, D. G.; Hyster, T. K., Accessing Non-Natural Reactivity by Irradiating Nicotinamide-Dependent Enzymes with Light. *Nature* **2016,** *540*, 414-417.
19. Kim, J.; Lee, S. H.; Tieves, F.; Choi, D. S.; Hollmann, F.; Paul, C. E.; Park, C. B., Biocatalytic C=C Bond Reduction through Carbon Nanodot-Sensitized Regeneration of NADH Analogues. *Angew. Chem., Int. Ed.* **2018,** *57*, 13825-13828.
20. Lazarides, T.; Sazanovich, I. V.; Simaan, A. J.; Kafentzi, M. C.; Delor, M.; Mekmouche, Y.; Faure, B.; Reglier, M.; Weinstein, J. A.; Coutsolelos, A. G.; Tron, T., Visible Light-Driven O_2 Reduction by a Porphyrin-Laccase System. *J. Am. Chem. Soc.* **2013,** *135*, 3095-3103.
21. Lee, S. H.; Choi, D. S.; Pesic, M.; Lee, Y. W.; Paul, C. E.; Hollmann, F.; Park, C. B., Cofactor-Free, Direct Photoactivation of Enoate Reductases for the Asymmetric Reduction of C=C Bonds. *Angew. Chem., Int. Ed.* **2017,** *56*, 8681-8685.
22. Liu, X.; Kang, F.; Hu, C.; Wang, L.; Xu, Z.; Zheng, D.; Gong, W.; Lu, Y.; Ma, Y.; Wang, J., A Genetically Encoded Photosensitizer Protein Facilitates the Rational Design of A Miniature

Photocatalytic CO_2-Reducing Enzyme. *Nat. Chem.* **2018,** *10*, 1201-1206.
23. Kang, F. Y.; Yu, L.; Xia, Y.; Yu, M. L.; Xia, L.; Wang, Y. C. A.; Yang, L.; Wang, T. Y.; Gong, W. M.; Tian, C. L.; Liu, X. H.; Wang, J. Y., Rational Design of a Miniature Photocatalytic CO_2-Reducing Enzyme. *ACS Catal.* **2021,** *11*, 5628-5635.
24. Wei, H.; Gao, L. Z.; Fan, K. L.; Liu, J. W.; He, J. Y.; Qu, X. G.; Dong, S. J.; Wang, E. K.; Yan, X. Y., Nanozymes: A Clear Definition with Fuzzy Edges. *Nano Today* **2021,** *40*, 101269.
25. Jiang, D.; Ni, D.; Rosenkrans, Z. T.; Huang, P.; Yan, X.; Cai, W., Nanozyme: New Horizons for Responsive Biomedical Applications. *Chem. Soc. Rev.* **2019,** *48*, 3683-3704.
26. Xu, X. J.; Wang, J. H.; Huang, R. L.; Qi, W.; Su, R. X.; He, Z. M., Preparation of Laccase Mimicking Nanozymes and Their Catalytic Oxidation of Phenolic Pollutants. *Catal. Sci. Technol.* **2021,** *11*, 3402-3410.
27. Zhang, L.; Zhang, L.; Deng, H.; Li, H.; Tang, W.; Guan, L.; Qiu, Y.; Donovan, M. J.; Chen, Z.; Tan, W., In Vivo Activation of pH-Responsive Oxidase-Like Graphitic Nanozymes for Selective Killing of Helicobacter Pylori. *Nat. Commun.* **2021,** *12*, 2002.
28. Li, N.; He, Y.; Lian, J.; Liu, Q. Y.; Zhang, Y. X.; Zhang, X., Hg^{2+} Significantly Enhancing the Peroxidase-Like Activity of H_2TCPP/ZnS/CoS Nanoperoxidases by Inducing the Formation of Surface-Cation Defects and Application for the Sensitive and Selective Detection of Hg^{2+} in the Environment. *Inorg. Chem.* **2020,** *59*, 18384-18395.
29. Zhou, Y.; Liu, C.; Yu, Y.; Yin, M.; Sun, J.; Huang, J.; Chen, N.; Wang, H.; Fan, C.; Song, H., An Organelle-Specific Nanozyme for Diabetes Care in Genetically or Diet-Induced Models. *Adv. Mater.* **2020,** *32*, e2003708.
30. Zhang, J.; Liu, J., Light-Activated Nanozymes: Catalytic Mechanisms and Applications. *Nanoscale* **2020,** *12*, 2914-2923.
31. Liu, Y.; Wang, X.; Wei, H., Light-Responsive Nanozymes for Biosensing. *Analyst* **2020,** *145*, 4388-4397.
32. Wang, C.; Wang, H.; Xu, B.; Liu, H., Photo-Responsive Nanozymes: Mechanism, Activity Regulation, and Biomedical Applications. *View* **2020,** *2*, 20200045.
33. Wang, H.; Yang, W.; Wang, X.; Huang, L.; Zhang, Y.; Yao, S., A CeO_2@MnO_2 Core–Shell Hollow Heterojunction as Glucose Oxidase-Like Photoenzyme for Photoelectrochemical Sensing of Glucose. *Sens. Actuators B Chem.* **2020,** *304*, 127389.
34. Wei, Z.; Yu, Y.; Hu, S.; Yi, X.; Wang, J., Bifunctional Diblock DNA-Mediated Synthesis of Nanoflower-Shaped Photothermal Nanozymes for a Highly Sensitive Colorimetric Assay of Cancer Cells. *ACS Appl. Mater. Interfaces* **2021,** *13*, 16801-16811.
35. Schneider, J.; Matsuoka, M.; Takeuchi, M.; Zhang, J.; Horiuchi, Y.; Anpo, M.; Bahnemann, D. W., Understanding TiO_2 Photocatalysis: Mechanisms and Materials. *Chem. Rev.* **2014,** *114*, 9919-9986.
36. Rajh, T.; Dimitrijevic, N. M.; Bissonnette, M.; Koritarov, T.; Konda, V., Titanium Dioxide in the Service of the Biomedical Revolution. *Chem. Rev.* **2014,** *114*, 10177-216.
37. Chen, M.; Zhou, H.; Liu, X.; Yuan, T.; Wang, W.; Zhao, C.; Zhao, Y.; Zhou, F.; Wang, X.; Xue, Z.; Yao, T.; Xiong, C.; Wu, Y., Single Iron Site Nanozyme for Ultrasensitive Glucose Detection. *Small* **2020,** *16*, e2002343.

38. Jin, L. Y.; Dong, Y. M.; Wu, X. M.; Cao, G. X.; Wang, G. L., Versatile and Amplified Biosensing through Enzymatic Cascade Reaction by Coupling Alkaline Phosphatase in Situ Generation of Photoresponsive Nanozyme. *Anal. Chem.* **2015,** *87*, 10429-10436.
39. Jiang, B.; Duan, D. M.; Gao, L. Z.; Zhou, M. J.; Fan, K. L.; Tang, Y.; Xi, J. Q.; Bi, Y. H.; Tong, Z.; Gao, G. F.; Xie, N.; Tango, A.; Nie, G. H.; Liang, M. M.; Yan, X. Y., Standardized Assays for Determining the Catalytic Activity and Kinetics of Peroxidase-Like Nanozymes. *Nat. Protoc.* **2018,** *13*, 1506-1520.
40. Kubo, W.; Tatsuma, T., Mechanisms of Photocatalytic Remote oxidation. *J. Am. Chem. Soc.* **2006,** *128*, 16034-16035.
41. Di Valentin, C.; Pacchioni, G.; Selloni, A., Electronic Structure of Defect States in Hydroxylated and Reduced Rutile TiO_2(110) Surfaces. *Phys. Rev. Lett.* **2006,** *97*, 166803.
42. Nosaka, Y.; Nosaka, A., Understanding Hydroxyl Radical (•OH) Generation Processes in Photocatalysis. *ACS Energy Lett.* **2016,** *1*, 356-359.
43. Park, H.; Goto, T.; Cho, S.; Nishida, H.; Sekino, T., Enhancing Visible Light Absorption of Yellow-Colored Peroxo-Titanate Nanotubes Prepared Using Peroxo Titanium Complex Ions. *ACS Omega* **2020,** *5*, 21753-21761.
44. Nosaka, Y.; Nosaka, A. Y., Generation and Detection of Reactive Oxygen Species in Photocatalysis. *Chem. Rev.* **2017,** *117*, 11302-11336.
45. Shen, X. M.; Wang, Z. Z.; Gao, X. F.; Zhao, Y. L., Density Functional Theory-Based Method to Predict the Activities of Nanomaterials as Peroxidase Mimics. *ACS Catal.* **2020,** *10*, 12657-12665.
46. Lei, Y.; Huang, X.; Zhao, C.; Jin, Y.; Xu, H., The Effect of DMPO on the Formation of Hydroxyl Radicals on the Rutile TiO_2(110) Surface. *Phys. Chem. Chem. Phys.* **2020,** *22*, 13129-13135.
47. Zheng, J. H.; Zhang, L., Incorporation of CoO Nanoparticles in 3D Marigold Flower-Like Hierarchical Architecture $MnCo_2O_4$ for Highly Boosting Solar Light Photo-Oxidation and Reduction Ability. *Appl. Catal. B Environ.* **2018,** *237*, 1-8.
48. Zhang, C. Y.; Jia, F. C.; Li, Z. Y.; Huang, X.; Lu, G., Plasmon-Generated Hot Holes for Chemical Reactions. *Nano Res.* **2020,** *13*, 3183-3197.
49. Imanishi, A.; Okamura, T.; Ohashi, N.; Nakamura, R.; Nakato, Y., Mechanism of Water Photooxidation Reaction at Atomically Flat TiO_2 (rutile) (110) and (100) surfaces: Dependence on Solution pH. *J. Am. Chem. Soc.* **2007,** *129*, 11569-11578.
50. Liu, Q.; Wan, K.; Shang, Y.; Wang, Z. G.; Zhang, Y.; Dai, L.; Wang, C.; Wang, H.; Shi, X.; Liu, D.; Ding, B., Cofactor-Free Oxidase-Mimetic Nanomaterials from Self-Assembled Histidine-rich Peptides. *Nat. Mater.* **2021,** *20*, 395-402.
51. Ohno, T.; Masaki, Y.; Hirayama, S.; Matsumura, M., TiO_2-Photocatalyzed Epoxidation of 1-Decene by H_2O_2 Under Visible Light. *J. Catal.* **2001,** *204*, 163-168.
52. Salvador, P., On the Nature of Photogenerated Radical Species Active in the Oxidative Degradation of Dissolved Pollutants with TiO_2 Aqueous Suspensions: A Revision in the Light of the Electronic Structure of Adsorbed Water. *J Phys. Chem. C* **2007,** *111*, 17038-17043.